

terial recrystallized to a finer grain size at 871 than at 927°C.)

These data suggest that, at least for Ti-6Al-4V, the test conditions (strain-rate and temperature) for achieving maximum superplasticity (elongation) are not necessarily the same as those indicated by the m tests. The elongation to failure at a given temperature is proportional to m , but this correlation is not necessarily maintained when comparing data at various temperatures.

1. A. K. Ghosh and R. A. Ayres: *Met. Trans. A*, 1976, vol. 7A, pp. 1589-91.
2. J. W. Edington: *Met. Technol.*, 1976, vol. 3, no. 3, pp. 138-50.
3. D. Lee and W. A. Backofen: *Trans. TMS-AIME*, 1967, vol. 239, pp. 1034-40.
4. D. A. Woodford: *Trans. ASM*, 1969, vol. 62, pp. 291-93.
5. C. H. Hamilton and G. W. Stacher: *Met. Progr.*, 1976, vol. 109, no. 3, pp. 34-37.
6. R. R. Boyer and J. Magnuson: Unpublished research, The Boeing Company, Seattle, WA, 1977.

Identification of a Fracture Mode: The Tearing Topography Surface

ANTHONY W. THOMPSON AND JAMES C. CHESNUTT

Fracture surfaces of metals have long been characterized as "brittle" or "ductile," according to their visual appearance; the former type has also been described as "crystalline" or "faceted," while the latter is often called "fibrous." With the use of higher magnification techniques of fracture examination, particularly replica transmission electron microscopy (TEM) and scanning electron microscopy (SEM), there have grown up a group of *microscopic* appearance types, often called fracture "modes." Among the early efforts to catalog these modes were those of Beachem and Pelloux¹ and Philips *et al.*,² currently there are available two rather comprehensive catalogs of this type.^{3,4*} All classify microscopic fracture details (par-

*Ref. 3 is currently available version of Ref. 2.

ticularly of tensile fractures) into four classical modes: intergranular, cleavage, quasi-cleavage, and microvoid coalescence (or dimpled) fractures. There is a consequent tendency⁴ to assign any particular fracture topography to one of these four modes, although it is often the case that the majority of a fracture surface is "ill-defined" in classical terms and one must search to find local areas which are adequately "representative" of the mode assigned.

What we describe in this communication is an additional mode of fracture, one with a characteristic appearance; such a distinctive appearance is the fundamental criterion for distinguishing fracture modes.^{1-3,5} This mode is often observed in steels and in alpha-beta titanium alloys, such as Ti-6Al-4V (Ti-6-4), but is

ANTHONY W. THOMPSON is Professor, Department of Metallurgy and Materials Science, Carnegie-Mellon University, Pittsburgh, PA 15213. JAMES C. CHESNUTT is Member of Technical Staff, Science Center, Rockwell International, Thousand Oaks, CA 91360.

Manuscript submitted December 21, 1978.

also present in other materials, as described below; we believe it has not been previously described as a distinct mode only because it is "nonclassical." The fracture surfaces appear to be formed by ductile or microplastic tearing on a very fine (submicron) scale, and accordingly we refer to the result as a "tearing topography surface," or TTS fracture. The mode is observed in tensile specimens and in compact tension specimens fractured under either rising or cyclic (fatigue) stress intensities.

Examples of the topography are shown in the figures. Figure 1 shows the fracture surface of HY-130 steel with a bainitic microstructure.⁶ At low magnifications, Fig. 1(a), the typical complex tearing appearance is evident, with a number of classical dimples also present. At higher magnification, Fig. 1(b), the particles which have nucleated dimples are visible, but much of the fracture area consists of microplastic tearing. Additional examples from another specimen of the same material are shown in Fig. 1(c) and (d). Other steel microstructures also exhibit TTS fracture under some conditions. Figure 2 gives examples from a eutectoid steel (similar to AISI 1080), in which fracture occurs across and through pearlite colonies, and from HY-130 with a martensitic microstructure;⁶ the similarity to Fig. 1 is evident.

The TTS appearance is also observed in alpha-beta titanium alloys. Figure 3(a) is an example drawn from STA (solution treated and aged) Ti-6-4, which contains primary alpha particles about 10 μm in diam in a matrix (about 70 vol pct) of fine Widmanstätten alpha and beta. These microstructural constituents are not evident on the fracture surface, as was verified by the "plateau etching" technique.⁷ An additional example from Ti-6-4 is shown in Fig. 3(b), in this case material water quenched from the beta-field to give a mixed microstructure of fine Widmanstätten alpha and martensite. Here some flat fracture across alpha plates is evident, but the tearing portion of the fracture surface has a TTS appearance. Additional examples occur in Ti-6Al-2Sn-4Zr-6Mo, Fig. 3(c) and (d). Figure 3(c) is material with a similar microstructure to the Ti-6-4 of Fig. 3(a) except for coarser secondary Widmanstätten alpha plates in the matrix; here the fracture may reflect fine tearing in and at boundaries of the plates.^{8,9} Note also the similar scale of the fracture surface features to Fig. 1(a). Finally, when this alloy is water quenched from the beta-field, analogously to the Ti-6-4 of Fig. 3(b), it again shows a typical TTS appearance (Fig. 3(d)).

Figure 4 is the fracture surface of a Ni-20 Cr-2 ThO₂ material;¹⁰ the fracture largely comprises fine dimples, but the fine scale tearing as well as the blocky aspect seen in some of the other TTS fractures is also evident. Figures 1 to 4, then, express the typical range of TTS appearance. In addition, there are many published fractographs* which contain TTS character; the

*Examples which appear to exhibit at least some areas of TTS appearance are as follows: steels (Figs. 3748, 3749, 3809, 3814, 3842, 3851, 3860, 4216, 4224, 4226, and 4297. Ref. 4), aluminum alloys (p. 4-87, Ref. 3; Figs. 3967, 4063, and 4071, Ref. 4), titanium alloys (p. 4-609, Ref. 3; Figs. 4177, 4185, 4193, 4195, and 4260 Ref. 4; Ref. 9), and nickel alloys (p. 4-664, Ref. 3; Figs. 3921, and 3933, Ref. 4).

best collections are in the fractography atlases^{3,4}. The TTS mode is most easily recognized in SEM photographs, due to their more evident three dimensionality,

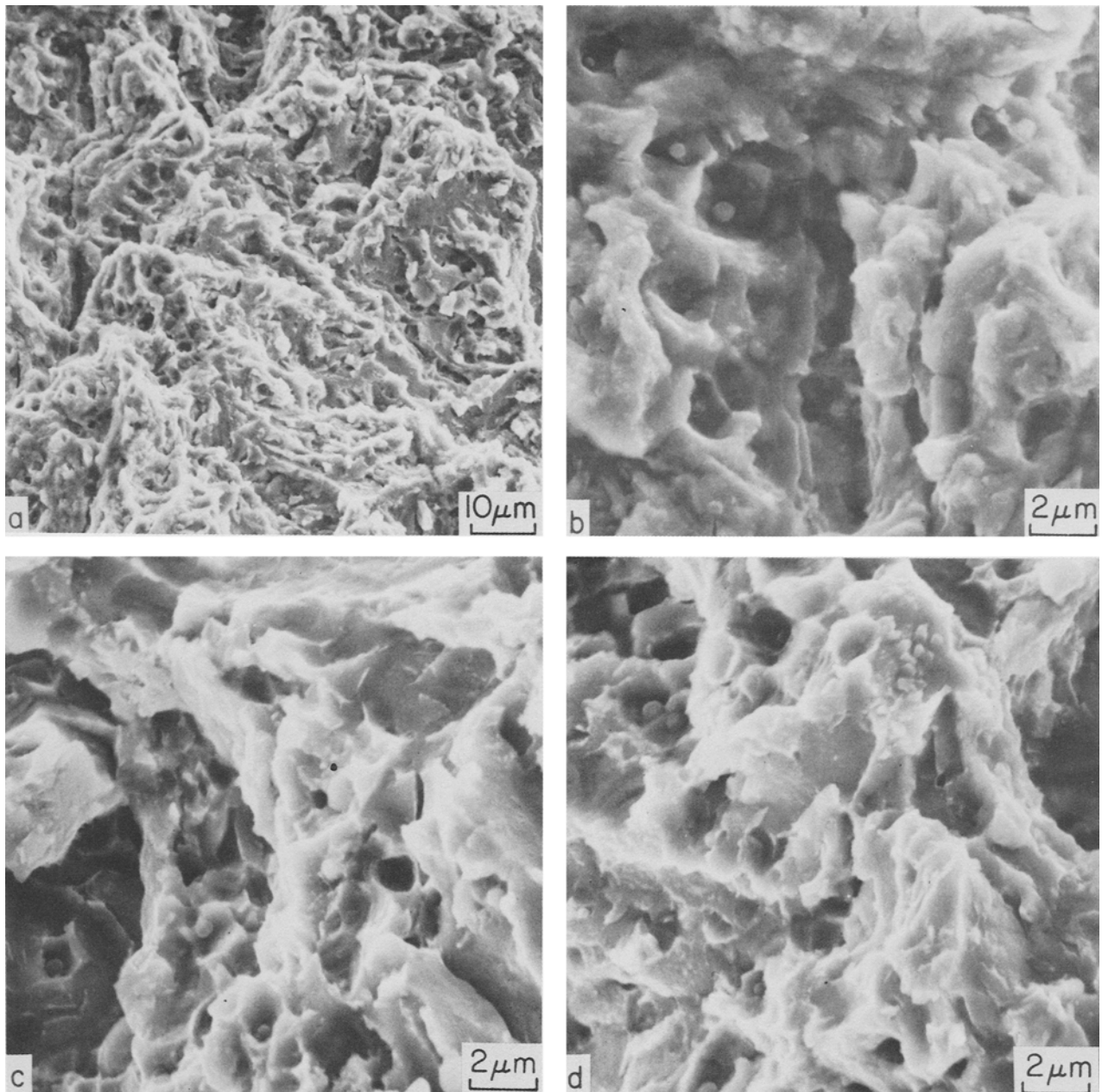


Fig. 1—Appearance of TTS fracture (SEM) in bainitic HY-130 steel: (a) Low magnification topography, (b) Detail from upper left corner of (a), showing apparent particle-nucleated dimples among fine tearing, (c) and (d) Other examples, again including some particles in dimples.

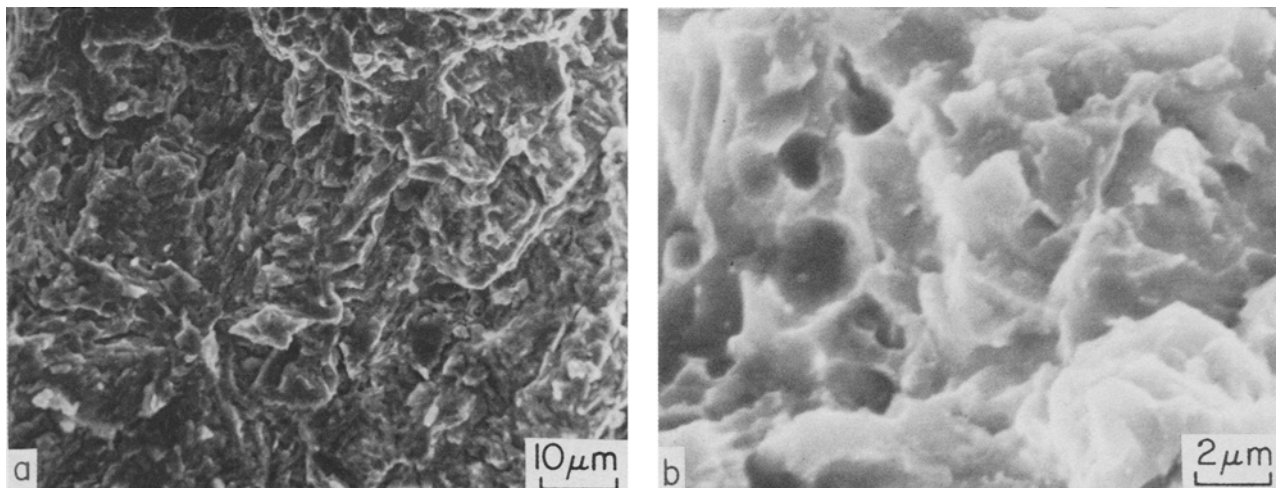


Fig. 2—Fracture surfaces (SEM) of other steel microstructures: (a) Eutectoid steel, essentially 100 pct pearlite, at low magnification, (b) Quenched and tempered (martensitic) HY-130 at higher magnification; compare Fig. 1(b), (c), and (d).

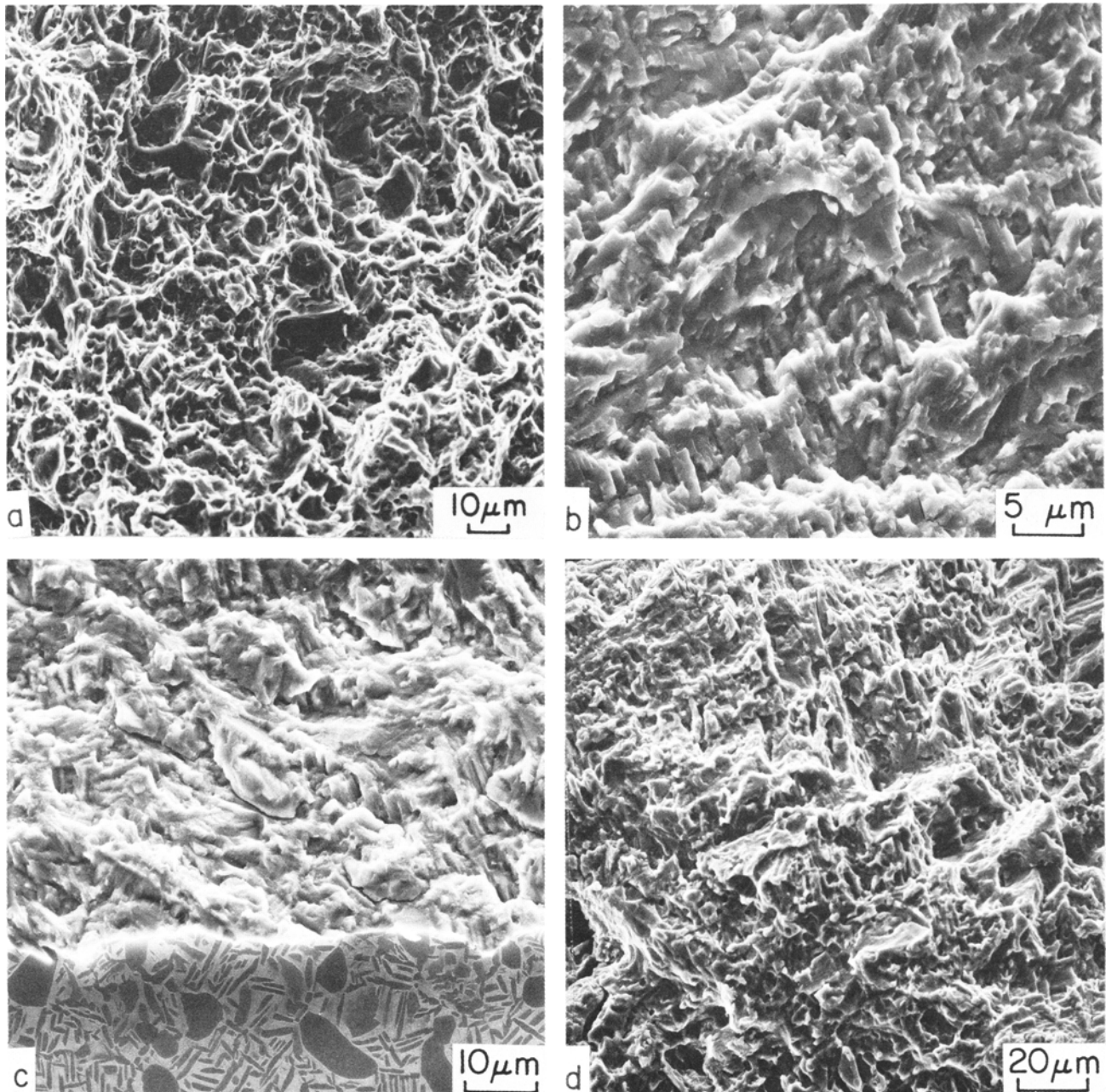


Fig. 3—Fracture appearance (SEM) in alpha-beta titanium alloys: (a) Ti-6-4 in STA condition, (b) Ti-6-4 in beta quenched condition, (c) Ti-6-2-4-6 in STA condition; specimen has been "plateau-etched",⁷ (d) Ti-6-2-4-6 in beta quenched condition.

but stereo viewing of replica TEM photos¹³ can provide equivalent information.

It is felt that although the microstructural nuclei for this fracture mode have not been identified (nuclei are also unknown for most examples of the other modes except dimpled fracture), the general appearance is distinct and not restricted to one alloy system. Furthermore, the generality of the mode is supported by its observation in tensile specimens (Figs. 2(a) and 4), and in compact tension specimens fractured under rising stress intensity (Figs. 1, 2(b) and 3(a)), or fatigue (Figs. 3(b) to (d)). Moreover, it occurs in the presence of hydrogen (Fig. 4(b)), as do each of the other modes.^{9,11,12,14}

It is possible that the TTS mode is a kind of microvoid coalescence in which very complex and closely

spaced nucleation occurs. (This would be consistent with the fact that nearly all the microstructures in which TTS fracture occurs contain high densities of interfaces which could serve as nuclei.) In this case, either the small amount of subsequent void growth or premature strain localization would prevent the observation of well-developed voids; this would be a parallel to the belief in some quarters that quasi-cleavage is merely a poorly developed cleavage mode. However, the observation, Fig. 1, of voids intimately mixed with the TTS areas tends to cast doubt on this view, as does the observation of the mode under varying stress states. As an empirical approach, therefore, it is proposed that the TTS mode be considered an independent fracture mode pending detailed investigation of nucleation and propagation processes.

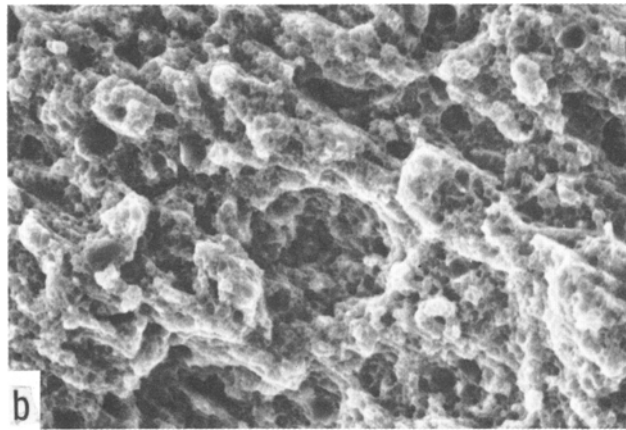
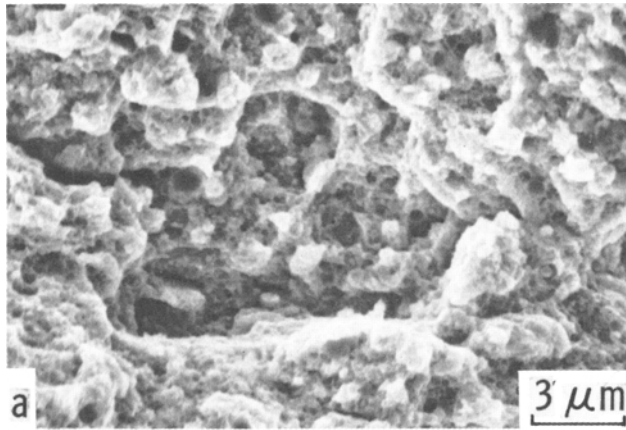


Fig. 4—Fracture surfaces (SEM) of Ni-20 Cr-2 ThO₂ fractured at room temperature.¹⁰ (a) Without hydrogen, (b) Hydrogen-charged, same magnification as (a).

We appreciate provision of unpublished fractographs by H. L. Gearhart and C. Chen, and assistance with nomenclature by J. C. Williams. This work was conducted as part of the Independent Research and Development Program of Rockwell International, when both authors were at the Science Center; subsequent participation of one of us (AWT) was supported by the National Science Foundation, Grant DMR 78-00723.

1. C. D. Beachem and R. M. N. Pelloux: *Fracture Toughness Testing and Its Applications* (STP 381), pp. 210-44, ASTM., Philadelphia PA, 1965.
2. A. Phillips, V. Kerlins, R. A. Rawe, and B. V. Whiteson: *Electron Fractography Handbook*, Report AFML-TR-64-416, Air Force Systems Command, Wright-Patterson AFB, Ohio, January 1965.
3. A. Phillips, V. Kerlins, R. A. Rawe, and B. V. Whiteson: *Electron Fractography Handbook*, MCIC-HB-08, Metals and Ceramics Inf. Center, Columbus, Metals and Ceramics Inf. Center, Columbus, OH, June 1976.
4. *Metals Handbook*, 8th ed., vol. 9, ASM, Metals Park, OH, 1974.
5. C. Crussard, R. Borione, J. Plateau, Y. Morillon, and F. Maratray: *J. Iron Steel Inst.*, 1956, vol. 183, pp. 146-77.
6. C. Chen, A. W. Thompson, and I. M. Bernstein: in press, *Oroc. 5th Bolton Landing Conf.*, Claitor's, Baton Rouge, LA.
7. J. C. Chesnutt and R. A. Spurling: *Met. Trans. A*, 1977, vol. 8A, pp. 216-18.
8. A. W. Thompson and J. C. Williams: *Fracture 1977*, vol. 2, pp. 343-48, Proc. 4th Int. Conf. on Fracture, Univ. Waterloo Press, Waterloo, Ontario, 1977.
9. A. W. Thompson and I. M. Bernstein: *Hydrogen in Metals*, vol. 10, paper 3A-6, Proc. 2nd Int. Congress, Pergamon Press, NY, 1977.
10. A. W. Thompson: *Met. Trans.*, 1974, vol. 5, pp. 1855-61.
11. A. W. Thompson: *Environmental Degradation of Engineering Materials*, pp. 3-17, VPI Press, Blacksburg, VA, 1977.
12. A. W. Thompson and I. M. Bernstein: *Fracture 1977*, vol. 2, pp. 249-54,

Proc. 4th Int. Conf. on Fracture, Univ. Waterloo Press, Waterloo, Ontario, 1977.

13. J. A. Fellows: *Metals Handbook*, 8th ed., vol. 9, pp. 281-96, ASM, Metals Park, OH, 1974.

14. A. W. Thompson: *Environment-Sensitive Fracture of Engineering Materials*, pp. 379-410, TMS-AIME, Warrendale, 1979.

Fractographic Characteristics of a Hydrogen-Charged AISI 316 Type Austenitic Stainless Steel

HANNU HÄNNINEN AND TERO HAKKARAINEN

It has been shown that the ductility of austenitic stainless steels is reduced by charging with hydrogen through cathodic polarization or in a hydrogen atmosphere,¹⁻⁴ but the basic fractographic features associated with hydrogen induced reduced ductility have not been established in detail. In the present work the hydrogen embrittlement of an AISI 316 steel (Table I) was studied by charging it with hydrogen through cathodic polarization and by subsequent tensile testing.

The tensile specimens (Fig. 1) were prepared by cold rolling a plate to the thickness of about 0.3 mm and then by cutting from the sheets. The specimens were annealed for 1 h at 1373 K in an evacuated silica tube and quenched into room temperature water. The subsequent thinning of the specimens was performed by grinding with emery paper with the final grinding being performed by 600 grit paper. The cathodic charging of the specimens was carried out at 353 K in a 1 N H₂SO₄ solution containing 0.25 g of NaAsO₂ per liter. A platinum counter electrode and a current density of 50 mA/cm² were used. The hydrogen charging time was 18 h. After charging, the specimens were tensile tested within 5 min at room temperature in a tensile testing machine at a crosshead speed of about 5 cm/min. After failure, the fracture surfaces were examined with a scanning electron microscope. Measurements to detect the possible hydrogen induced α' -martensite were made on the faces of the specimens as near as possible to the main crack using a ferrite detector (Ferritescope) with a sensitivity of 0.1 vol pct of α' -martensite.

The fracture stress of a hydrogen charged AISI 316 steel specimen was 97 N/mm² and no elongation to fracture could be detected. For a similar uncharged reference specimen the yield strength was 300 N/mm², the fracture stress was 477 N/mm², and the elongation to fracture was 30 pct. Minor surface cracking was observed after tensile testing on the outer surfaces of the hydrogen charged specimens. The surface cracking occurred in part during charging, but during room temperature aging after charging the surface cracking increased markedly as ob-

HANNU HÄNNINEN and TERO HAKKARAINEN are Scientist and Research Professor, respectively, Technical Research Centre of Finland, 02150 Espoo 15, Finland.

Manuscript submitted November 20, 1978.